Renewable Energy 80 (2015) 610–628

Contents lists available at ScienceDirect

Renewable Energy

journal homepage: www.elsevier.com/locate/renene

A database of capture width ratio of wave energy converters

A. Babarit

LHEEA Lab, Ecole Centrale de Nantes – CNRS, 1 rue de la Noe, 44300 Nantes, France

ARTICLE INFO

Article history:
Received 25 September 2014
Accepted 22 February 2015
Available online

Keywords:
Wave energy converter
Capture width ratio
Hydrodynamic efficiency
Database

ABSTRACT

The aim of this study is to establish a database for the hydrodynamic performance of Wave Energy Converters (WECs). The method relies on the collection and analysis of data available in the literature. The availability and presentation of these data vary greatly between sources. Thus, extrapolations have been made in order to derive an annual average for the capture width ratio (CWR) of the different technologies. These CWR are synthesized in a table alongside information regarding dimension, wave resource and operational principle of the technologies. It is observed that CWR is correlated to operational principle and dimension. Statistical methods are used to derive relationships between CWR and dimension for the different WEC operational principles.

1. Introduction

Since the early 1980s, hundreds of Wave Energy Converters (WECs) have been studied and developed. Full-scale prototypes have been tested, and technology review papers have been published (see for example [1–8]). These papers usually discuss the technologies, their classifications and technical aspects (e.g. the Power Take-off (PTO) system). They do not discuss power performance of the different wave energy technologies.

Information on power performance can be found in the literature, however in general, the information provided by any given paper is limited to the one technology being investigated. A few studies have compared power performance between different technologies, but they cover a limited number of devices [9–12].

Thus, the aim of this paper is to create an extensive database for the hydrodynamic performance of WECs by reviewing power performance results available in the public literature. In this paper, the approach elaborates and extends on the work by Ref. [13]. Power performance is quantified in terms of capture width ratio (CWR), which is reported for each device in Tables 7–9. To identify trends, the results were classified according to WEC operational principle. A relationship between dimension and CWR was identified and discussed in the last part of this paper.

It must be acknowledged that making an objective comparison of CWR across WEC technologies is not an easy task. In this work, it has been necessary to make assumptions and approximations in order to address issues related to discrepancies in the collected data. These are discussed in Section 2 and Section 4, and are believed to be reasonable. However, it is nevertheless possible that they may influence the final results in Section 4. Since all assumptions and approximations made have been described in detail in this paper, the extent of this influence may be assessed in future work.

2. Methods

The sources for the present work are references [9–11] and [14–45], which present performance results for various WECs. The performance measure used and the way in which results are presented vary greatly from one source to another. Thus, for the purpose of comparison, it was necessary to select a common performance measure, namely annual average of CWR. Note that CWR may also be referred to in the literature as "'non-dimensional performance"' [12].

2.1. CWR

Capture width (CW) was first introduced in 1975 by Ref. [46]. It is defined as the ratio of absorbed wave power P (in kW) to the wave resource J (in kW/m):

$$CW = \frac{P}{J} \tag{1}$$

The unit of capture width is a length in metres. It may be

E-mail address: aurelien.babarit@ec-nantes.fr.

http://dx.doi.org/10.1016/j.renene.2015.02.049
0960-1481/

Table 1
Summary of performance results for the WEPTOS technology studied in Refs. [32–34].

Technology	Operational principle	η_1	Dimension (m)		Resource (kW/m)
WEPTOS	Variation of fixed OWSC	8	2.9	Width	6
		10	2.9	Width	16
		12	3.6	Width	6
		12	3.6	Width	16
		19	4.8	Width	6
		15	4.8	Width	16
		15	5.4	Width	9
		25	6.0	Width	6
		19	6.0	Width	16
		32	8.3	Width	16
		22	9.6	Width	29
		25	9.6	Width	26

Table 2
Performance results for technologies studied in Ref. [43].

Technology	Operational principle	η_1	Dimension (m)		Resource (kW/m)
NEL Terminator	OWC	55	22	Width	30
NEL Floating Terminator	OWC	24	22	Width	54
NEL Floating Attenuator	OWC	41	20	Width	54
Vicker's Terminator	Variant of OWC	34	30	Width	36
Vicker's Attenuator	Variant of OWC	16	30	Width	36
Belfast Point Absorber	Variant of OWC	35	29	Outer diameter	42
Edinburgh Duck	Variant of OWSC	47	37	Width	54
Bristol Cylinder	Variant of OWSC	46	75	Width	48
Lancaster Flexible Bag	Variant of OWSC	9	20	Width	51
Lanchester Clam	Variant of OWSC	23	27	Width	51

interpreted as the width of wave crest that has been completely captured and absorbed by the WEC.

More than capture width, it is hydrodynamic efficiency that best reflects the hydrodynamic performance of a WEC. A measure of the hydrodynamic efficiency is the CWR, obtained by dividing the capture width by a characteristic dimension B of the WEC – often the device width. CWR, denoted by η_1, reflects the fraction of wave power flowing through the device that is absorbed by the device:

$$\eta_1 = \frac{CW}{B} = \frac{P}{JB} \tag{2}$$

Table 3
Performance results for technologies studied in Ref. [9].

Technology	Operational principle	η_1	Dimension (m)		Resource (kW/m)
Swan DK3	OWC	20	16	Width	16
Bølgehovlen	Overtopping	8	10	Diameter	16
Power pyramid	Variant of overtopping	12	125	Width	16
Wavedragon	Overtopping	23	259	Width	16
Sucking Sea Shaft	Variant of overtopping	3	125	Width	16
Bølgepumpen	Variant of heaving device	6	5	Diameter	16
Point absorber	Heaving device	14	10	Diameter	16
DWP system	Heaving device	20	10	Diameter	16
Tyngdeflyderen	Variant of heaving device	12	30	Characteristic diameter	16
Wave plunger	Variant of fixed OWSC	16	15	Width	16
Poseidon	Unknown	27	420	Width	16
Bølgeturbinen	Wave turbine	4	15	Rotor diameter	16

Table 4
Performance results for technologies studied in Ref. [10].

Technology	Operational principle	η_1	Dimension (m)		Resource (kW/m)
AquaEnergy/ AquaBuOY	Heaving device	[10–26]	6	Diameter	[12–26]
Energetech	OWC	58	35	Width	[12–26]
INRI/SEADOG	heaving device	[16–24]	5.7	Diameter	[12–26]
Ocean Power Delivery/ Pelamis	Variant of heaving device	[14–21]	15	Characteristic diameter	[12–26]
ORECON/MR1000	OWC	[176–281]	32	Diameter	[12–26]
TeamWork/AWS	Variant of heaving device	[138–205]	9.5	Diameter	[12–26]
Wavebob	Heaving device	[40–51]	15	Diameter	[12–26]
Wavedragon	Overtopping	[21–26]	24	Width	[12–26]

Table 5
Performance results for technologies studied in Ref. [11].

Technology	Operational principle	η_1	Dimension (m)		Resource (kW/m)
Small bottom-referenced heaving buoy	Variant of heaving device	[3–4]	3	Diameter	[15–37]
Bottom-referenced submerged heave-buoy	Heaving device	[8–13]	7	Diameter	[13–34]
Floating-two body heaving converter	Heaving device	[27–36]	20	Diameter	[15–37]
Bottom-fixed heave-buoy array	Heaving device	[12–17]	5	Diameter	[13–34]
Floating heave-buoy array	Heaving device	[6–11]	8	Diameter	[15–37]
Bottom-fixed oscillating flap	Fixed OWSC	[58–72]	26	Width	[13–34]
Floating three-body oscillating flap	Floating OWSC	[7–13]	19	Width	[15–37]
Floating OWC	OWC	[22–35]	24	Width	[15–37]

Selection of a relevant characteristic dimension for B is critical in order to make CWR comparable between different wave energy devices. This is discussed further in Section 2.4.

It is important to note that CWR relates to hydrodynamic power performance (energy absorption) and not economical performance (cost of energy). Efficiency in the PTO system and the power conversion chain, as well as fabrication and operation costs, may be such that the most efficient device hydrodynamically speaking

Table 6
Performance results for technologies studied in Ref. [44].

Technology	Operational principle	Mean absorbed power per flap	η_1	Dimension (m)		Resource (kW/m)
Vertical flaps on fixed supporting frame	Variant of fixed OWSC	240	31	25	Width	30
		450	37	50		
		220	30	25		
Vertical flaps on supporting frame with taut moorings	Floating OWSC	138	18	25	Width	30
		266	18	50		
Vertical flaps on supporting frame with slack moorings	Floating OWSC	58	8	25	Width	30
		128	8	50		
		158	21	25		

Table 7
Summary table of energy performance of wave energy converters.

Category	Technology	η_1 (%)	Resource (kW/m)	Characteristic dimension(m)		Ref.	Methods	Source
Oscillating Water Column	NEL Terminator	55	30	22	Width	[43]	Model tests	Independent
	NEL Floating Terminator	24	54	22	Width	[43]	Model tests	Independent
	NEL Floating Attenuator	41	54	20	Width	[43]	Model tests	Independent
	Swan DK3	20	16	16	Width	[9]	Model tests	Independent
	Energetech	72	12	35	Width	[10]	N/A	Developer
		58	21					
		58	26					
		33	15					
	ORECON/MR1000	*213*	*12*	*32*	*Diameter*	[10]	*N/A*	*Developer*
		209	*21*					
		176	*26*					
		281	*15*					
	Floating OWC	23	15	24	Width	[11]	N/A	Independent
		32	22					
		35	27					
		24	37					
	NEL-OWC	22	16	30	Width	[14]	Sea trials	Developer
		27	23					
		29	27					
		23	37					
	Mutriku wave power plant	7	26	6	Width	[15]	Model tests	Developer
	Pico	20	38	12	Width	[17]	Prototype	Independent
Variant of oscillating water column	Vickers Terminator	34	36	30	Width	[43]	Model tests	Independent
	Vickers Attenuator	16	36	30	Width	[43]	Model tests	Independent
	Belfast Point absorber	35	42	29	Diameter	[43]	Model tests	Independent
	Floating	17		8	Diameter	[16]	Numerical modelling	Independent
		23	31	12				
	KNSWING	18	14	7.5	Width	[18]	Model tests	Developer
	Floating OWC	12	15	12.5	Width	[19]	Model tests	Independent
		14	23					
		15	27					
		12	36					
Overtopping devices	Bolgehovlen	8	16	10	Diameter	[9]	Model tests Independent	
	Wavedragon	23	16	259	Width	[9]	Model tests	Independent
	Wavedragon	26	12	300	Width	[10]	N/A	Developer
		23	21					
		21	26					
		22	15					
	Wavedragon	27	6	65	Width	[21]	Model tests	Developer
		18		97				
Variant of overtopping devices	Power pyramid	12	16	125	Width	[9]	Model tests	Independent
	Sucking Sea Shaft	3	16	125	Width	[9]	Model tests	Independent
	SSG	23	19.5	10	Width	[20]	Model tests	Developer

could be the least efficient device from the perspective of cost of energy.

2.2. Harmonization of power performance results

Only a few of the sources present data for the annual average of capture width and wave resource *J*. In other cases, it is necessary to extrapolate from available results to estimate CWR. The methodology is illustrated in Fig. 1 and discussed in the following.

In some of the sources, power matrices are provided. In these cases, estimates of annual average capture width at different locations are obtained by first multiplying scatter diagrams with power matrices and then summing the power contributions from each sea state. Scatter diagrams shown in Ref. [11] were used. Linear interpolation is when the bins of the power matrix and the scatter diagram do not match.

In other sources, information about capture width or power absorption is provided for only a limited number of sea states. In these cases, it is necessary to estimate the power matrices as follows. First, it was assumed that power absorption is zero for sea states with peak period less than 3 s or greater than 20 s. Then, linear interpolation was used to obtain power absorption as a function of the peak period. Finally, the power matrix was fully populated by scaling power absorption with the square of significant wave height. Once the power matrix was derived, annual average capture width was calculated using the methodology explained in the previous paragraph.

Still other sources provide information on performance only in regular waves. In these cases, power matrices were generated, again assuming linearity. Power absorption in regular waves was obtained by integrating over frequency the product of Jonswap spectrum with the power absorption in regular waves. Once the power matrix was determined, annual average of capture width was determined as explained previously.

Finally, some sources provide data on power absorption with and without advanced control (e.g. latching control, in the case of source [22]). Only power absorption with passive control was retained in the database. This was essentially for the sake of consistency, but also because many practical challenges remain to be solved before advanced control is feasible [47–49].

2.3. Classification of technologies

WEC technologies may be classified by: their dimension and arrangement with respect to the main wave direction; their distance to shore; or their operational principle. One of the most

Table 8
Summary table of energy performance of wave energy converters (continued).

Category	Technology	η_1 (%)	Resource (kW/m)	Characteristic dimension(m)		Ref.	Methods	Source
Heaving devices	Point absorber	14	16	125	Width	[9]	Model tests	Independent
	DWP system	20	16	10	Diameter	[9]	Model tests	Independent
	AquaEnergy/AquaBuOY	20	12	6	Diameter	[10]	N/A	Developer
		17	21					
		14	26					
		21	15					
	INRI/SEADOG	24	12	5.7	Diameter	[10]	N/A	Developer
		16	21					
		16	26					
		21	15					
	Wavebob	40	12	15	Diameter	[10]	N/A	Developer
		51	21					
		46	26					
		45	15					
	Small bottom-referenced heaving buoy	4	15	3	Diameter	[11]	Numerical modelling	Independent
		4	22					
		4	27					
		3	37					
	Floating two-body heaving converter	27	15	20	Diameter	[11]	Numerical modelling	Independent
		29	22					
		36	27					
		27	37					
	Bottom-fixed heave-buoy array	14	13	5	Diameter	[11]	Numerical modelling	Independent
		16	19					
		17	22					
		12	34					
	Floating heave-buoy array	11	15	8	Diameter	[11]	Numerical modelling	Independent
		11	22					
		11	27					
		6	37					
	Two-body heaving device	25	31	15	Diameter	[45]	Numerical modelling	Independent
	Hydrocap/SEACAP	*4*	*25*	*10*	*Diameter*	[22]	*Numerical modelling*	*Independent*
		3		*11*				
		6		*15*				
		6		*16.5*				
		9		*20*				
	Inspired by OPT LifeSaver	19	40	10	Diameter	[23]	Numerical modelling	Independent
		12.5	27	12.5	Diameter	[25]	Prototype	Developer
	Inspired by Wavestar	10	N/A	4	Diameter	[26]	Numerical modelling	Independent
		15	15					
	Lifesaver	12	26	12.5	Characteristic diameter	[25]	Prototype	Developer
	RM3	16	34	20	Diameter	[27]	Numerical modelling	Independent
Variant of heaving devices	Bolgepumpen	6	16	5	Diameter	[9]	Model tests	Independent
	Tyngdeflyderen	12	16	30	Characteristics diameter	[9]	Model tests	Independent
	Pelamis	21	12	15	Characteristic diameter	[9]	N/A	Developer
		15	21					
		14	26					
		18	15					
	AWS	*138*	*12*	*9.5*	*Diameter*	[10]	*N/A*	*Developer*
		205	*21*					
		142	*26*					
		145	*15*					
	Bottom-referenced submerged heave-buoy	9	13	7	Diameter	[11]	Numerical modelling	Independent
		13	19					
		13	22					
		8	34					
	DEXA	8	26	22	Characteristic diameter	[24]	Model tests	Independent

representative classifications on the basis of operational principle was proposed by Falcão [4]. In this classification, devices are grouped into three main categories: oscillating water columns (OWCs), overtopping devices or oscillating bodies (referred to as wave-activated bodies in Ref. [4]). Since oscillating bodies covers a broad range of devices, this category was divided further into floating or bottom fixed devices (the latter referred to as "submerged" in Ref. [4]); and Oscillating Wave Surge Converters (referred to as "essentially rotation" in Ref. [4]) or heaving devices (referred to as "essentially translation (heave)" in Ref. [4]). In this work, we follow the same classification, except that no distinction is made between floating and bottom-fixed heaving devices. Thus, oscillating bodies are classified as either heaving devices (devices moving essentially in heave), fixed OWSCs (OWSCs attached to a fixed reference), or OWSCs attached to a floating reference.

For oscillating bodies, it is believed that this distinction between heaving and surging devices has to be made because the direction of motion is an important parameter for hydrodynamic

Table 9
Summary table of energy performance of wave energy converters (continued).

Category	Technology	η_1 (%)	Resource (kW/m)	Characteristic dimension(m)		Ref.	Methods	Source
Fixed OWSC	Bottom-fixed	61	13	26	Width	[11]	Numerical modelling	Independent
	oscillating flap	68	19					
		72	22					
		58	34					
	Bottom-fixed	49	18	25.5	Width	[45]	Numerical modelling	Independent
	oscillating flap							
	Biopower	45	38.5	6.6	Diameter	[30]	Model tests	Developer
	OWSC	35	N/A	6	Width	[31]	Model tests	Developer
		52		12				
		62		18				
		65		24				
	Inspired by	22	26	6	Width	[35]	Numerical modelling	Independent
	Oyster	40		12				
		55		18				
	Surface piercing	17	26	5	Width	[38]	Numerical modelling	Independent
	flap	36		10				
		72		20				
		64		50				
Variant of fixed OWSC	Edinburgh Duck	47	54	37	Width	[43]	Model tests	Independent
	Bristol Cylinder	46	48	75	Width	[43]	Model tests	Independent
	Lancaster flexible bag	9	51	20	Width	[43]	Model tests	Independent
	Lanchester Clam	23	51	27	Width	[43]	Model tests	Independent
	Wave plunger	16	16	15	Width	[9]	Model tests	Independent
	Vertical flaps on fixed	31	25	30	Width of	[44]	Numerical modelling	Independent
	supporting frame	37	50		each flap			
		30	25					
	Top-hinged flaps	25	25	12	Width	[29]	Model tests	Independent
	WEPTOS	10	16	2.9	Width	[32–34]	Model tests	Independent
		12	16	3.6				
		15	16	4.8				
		15	9	5.4				
		19	16	6				
		32	16	8.3				
		25	26	9.6				
	Combined wind and	45	26	16	Width	[36]	Numerical modelling	Independent
	wave energy platform							
	Combined wind and	61	26	9	Width	[37]	Numerical modelling	Independent
	wave energy platform							
Floating OWSC	Floating three-body	9	15	19	Width	[11]	Numerical modelling	Independent
	oscillating flap	13	22					
		13	27					
		7	37					
	Vertical flaps on	18	25	30	Width	[44]	Numerical modelling	Independent
	supporting frame	18	50					
	with taut moorings							
	Vertical flaps on	8	25	30	Width	[44]	Numerical modelling	Independent
	supporting frame	8	50					
	with slack moorings	21	25					
	Langlee	7	16	25	Width	[39,40]	Model tests	Independent
		5	21	25				
		9	16	37.5				
		9	16	50				
		10	21	50				
		10	21	100				
Variant of floating OWSC	Wavepiston	15	12	15	Width	[41]	Model tests	Independent
		8	3.5					
	SEAREV G1	20	25	13.6	Width	[42]	Numerical modelling	Developer
	SEAREV G21	16		30				
	SEAREV G3	25		30				

performance. Indeed, a well-known remarkable result in wave energy conversion is that, under certain assumptions, CWR relates only to the wavelength and the degree of freedom of the device [50], and not to its physical dimensions. Assuming (i) that linear potential flow theory is applicable and (ii) an axisymmetrical WEC (iii) with optimal reactive control, the theoretical maximum for the capture width is:

$$CW_{max} = \varepsilon \frac{\lambda}{2\pi} \tag{3}$$

where λ is the wavelength and ε is a coefficient dependent on the pattern of the radiated wave far field, and thus on the degree of freedom. If the system is moving in heave (heaving buoy), the far field component of the radiated waves has a circular pattern (left figure in Fig. 2) and the coefficient ε is equal to 1. If the system is moving in surge and/or pitch, the wave pattern is antisymmetric (right figure in Fig. 2) and the coefficient ε is 2. The theoretical maximum for wave absorption of an axisymmetric WEC moving in surge or pitch is twice that of for the same WEC moving in heave.

These theoretical results highlight the importance of the radiated wave pattern on the hydrodynamic performance of a WEC;

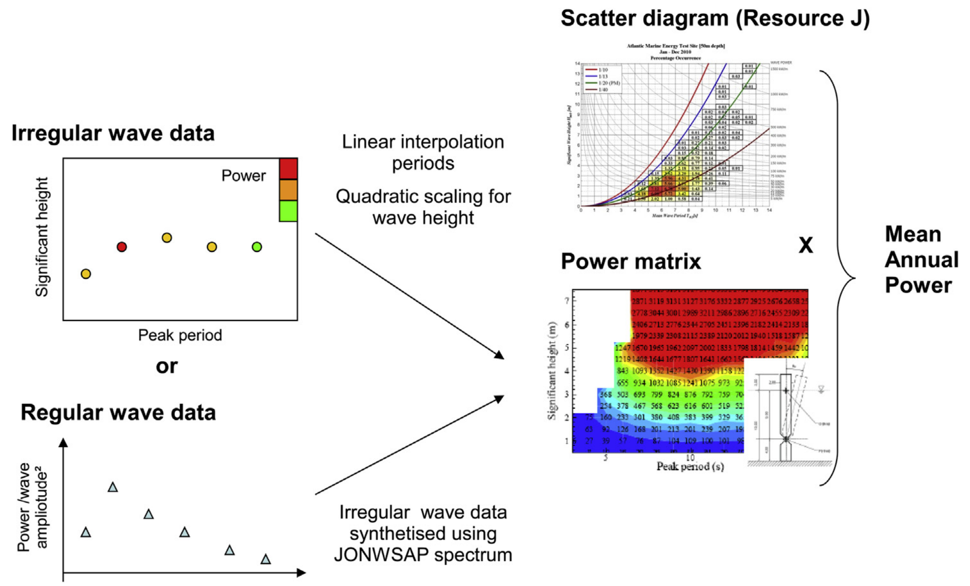

Fig. 1. Outline of the methodology used for the harmonization of power performance results.

hence, a WEC classification should take into account the WEC's far field radiated wave pattern. As this pattern is essentially related to the direction of motion, it represents a distinction between heaving devices and OWSCs. The latter have been further subdivided into devices attached to a fixed reference or a floating reference. Indeed, performance of floating OWSCs is considerably less than devices held to a fixed reference because the whole platform has a tendency to move as a rigid body instead of developing relative motion.

Fig. 3 shows the archetypal device for each category. It must be acknowledged that in practice, devices may differ significantly from the archetype. In some examples, the operational principle may be the only relationship between the device and the archetype. Thus, it was decided to sub-divide each category into those devices that are close realizations of the archetype, and those devices that are related to the category essentially by the operational principle. This distinction leaves us with the following ten categories: OWCs, variants of OWCs, overtopping devices, variants of overtopping devices, heaving devices, variants of heaving devices, fixed OWSCs, variants of fixed OWSCs floating OWSCs and variants of floating OWSCs.

Note that, in this study, articulated devices such as the Pelamis or the DEXA are classified as variants of heaving devices. This is because: (i) to first order, the motion of the centre of the floats is vertical, and (ii) from the hydrodynamical perspective, they can be approximated as a series of heaving buoys [51].

Most WECs proposed so far fall into one of these ten categories. However, there are exceptions, such as wave turbines [52,53] or flexible devices [54,55]. These have not been considered in this study because the available information is much more limited than for the other ten categories.

2.4. Selection of the characteristic dimension

For all except heaving devices, active width was used as the characteristic dimension, *B*, for calculating the CWR. The definition of [12] for the active width was followed, which is based on the idea that "(…) width of all the components actively in the primary absorption process of the energy from the waves should be included". Thus, in the case of a device composed of a platform with many WECs attached to it, the performance was normalized by the number of WECs on the platform and the active width was the width of each individual WEC. In the case of devices with reflectors or a wave concentration mechanism, the active width includes the reflectors. In the case of devices inclined relative to the incoming waves, the real (not projected) width was taken into account.

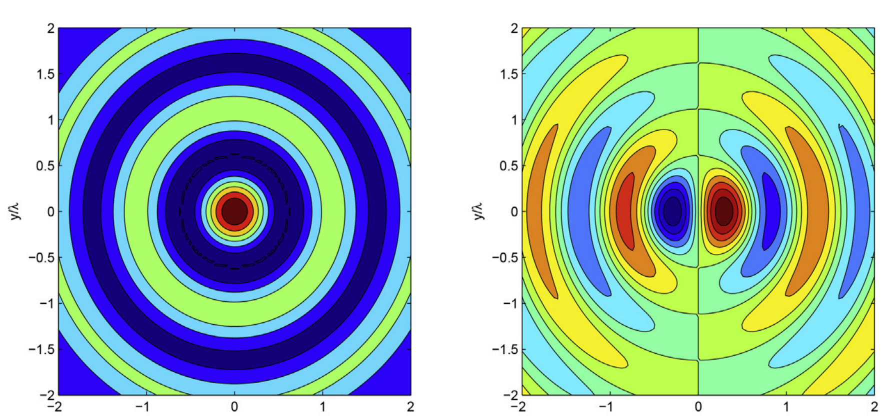

Fig. 2. Far field pattern of the radiated wave for an axisymmetric device moving in heave (left graph) and in surge (right figure).

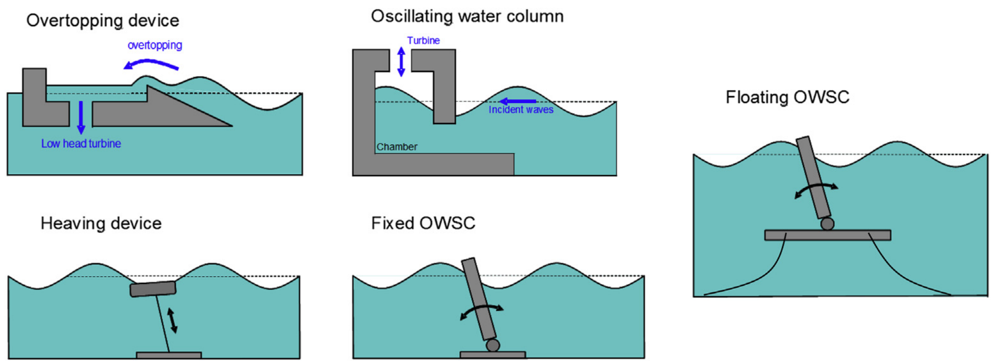

Fig. 3. Illustration of the archetypal wave energy device for each category.

For heaving devices, the characteristic diameter is obtained according to:

$$B = \sqrt{\frac{4A_W}{\pi}} \tag{4}$$

where A_W is the maximum horizontal cross-sectional area of the device, assumed to be the main driver for the ability of a heaving device to generate waves (and thus absorb waves [1]). Note that for vertical cylinders or floating hemispheres, A_W is simply equal to the diameter.

2.5. Additional information added to the database

The methodology used to derive the power performance results is important information to collect and retain in the database. Depending on the sources, numerical or experimental modelling has been used. For experimental modelling, the scale varies from small-scale to full-scale prototype. This information was included in the database.

Performance results may have been obtained by technology developers or third parties. This information was also collected and retained in the database, as occasionally performance results from technology developers may be suspected of unreliability due to conflicting interests.

3. Review of power performance results

3.1. List and discussion of sources

In this section, the sources used to compile the database are presented and discussed.

3.1.1. Oscillating water columns

Pictures of the OWC technologies discussed in this section are shown in Fig. 4.

- Ref. [14] reports experimental performance results for the NEL-OWC, which is a floating terminator device composed of several OWC modules mounted on a spine. The device was tested at large scale in the Solent with three, five and eight modules, each module having width of 1.5 m. Figure 11 of the paper presents CWR measured during the sea trials as a function of the energy period. The large spread of the sea trial results can be attributed to the varying properties of the waves. The eight module configuration gave best performance so was selected by us for estimation of the mean annual CWR. Assuming that the scale of the model was 1/20, we estimated mean annual CWR to be respectively 22, 27, 29, 23% for sites with wave resource 16, 23, 27, 37 kW/m.
- Ref. [15] deals with the design and construction of the Mutriku wave power plant, which is a combination of a breakwater with OWCs. The width of each OWC chamber is 6 m. Power performance was assessed through experiments on a 1/40 scale model of the plant, from which annual average pneumatic power capture was estimated to be 175 kW for the whole plant. The offshore wave resource being 26 kW/m, the mean annual CWR is 7%.
- Ref. [16] deals with performance optimization of a floating OWC using numerical modelling. Three configurations were investigated: (A) 8 m diameter and 24 m draft, (B) 8 m diameter and 36 m draft, (C) 12 m diameter and 24 m draft. Other dimensions and PTO characteristics were numerically optimized to maximize power absorption for a site offshore Portugal. The wave resource is 31 kW/m. Mean CWR is respectively 17%, 23% and 21% for configurations A,B and C (see Table 3 of the paper). As seen in Fig. 4, this device differs from the archetypal OWC in Fig. 3. Thus, it was included in the database as an OWC variant.
- Ref. [17] presents power performance results for the OWC pilot plant installed in Pico island in the Azores. Data had been collected from 2005 to 2010, during which period the plant had been running for approximately 1700 h in total. As reported in the source, the mean electrical power was measured to be 28 kW for an offshore wave resource of 38 kW/m. The efficiency of the Wells turbine was estimated to be 31%. The width of the plant is 12 m, thus the mean annual CWR is 20%.
- Ref. [18] presents results of experiments conducted in Cork (Ireland) for the KNSWING WEC. This device is an attenuator equipped with forty OWC chambers (twenty on the port side and twenty on starboard). The model scale is 1/50, with a length of 3 m. It was tested both in regular and irregular waves. Using this data and the scatter diagram provided in the report, we calculated the mean annual CWR to be 18% for a 7.5 m wide OWC and a 14 kW/m wave resource. The device was classified as variant of OWC because the OWC chambers are not facing the incident waves, see Fig. 4.
- Ref. [19] presents power performance results for a large V-shaped floating WEC developed in Ireland. Each arm of the V hosts sixteen OWC chambers. Power absorbed in each OWC chamber is manifolded and drives one single air turbine. The length of each arm is 250 m at full scale. A 1/50 scale model was tested in Cork, in Ireland. Figure 24 of the paper shows the performance of the technology in regular waves. Using this data, we estimated the mean annual CWR to be respectively 12, 14, 15, 12% for sites with wave resource 15, 23, 27, 36 kW/m. The device was classified as variant of OWC because the OWC chambers are not facing the incident waves, see Fig. 4.

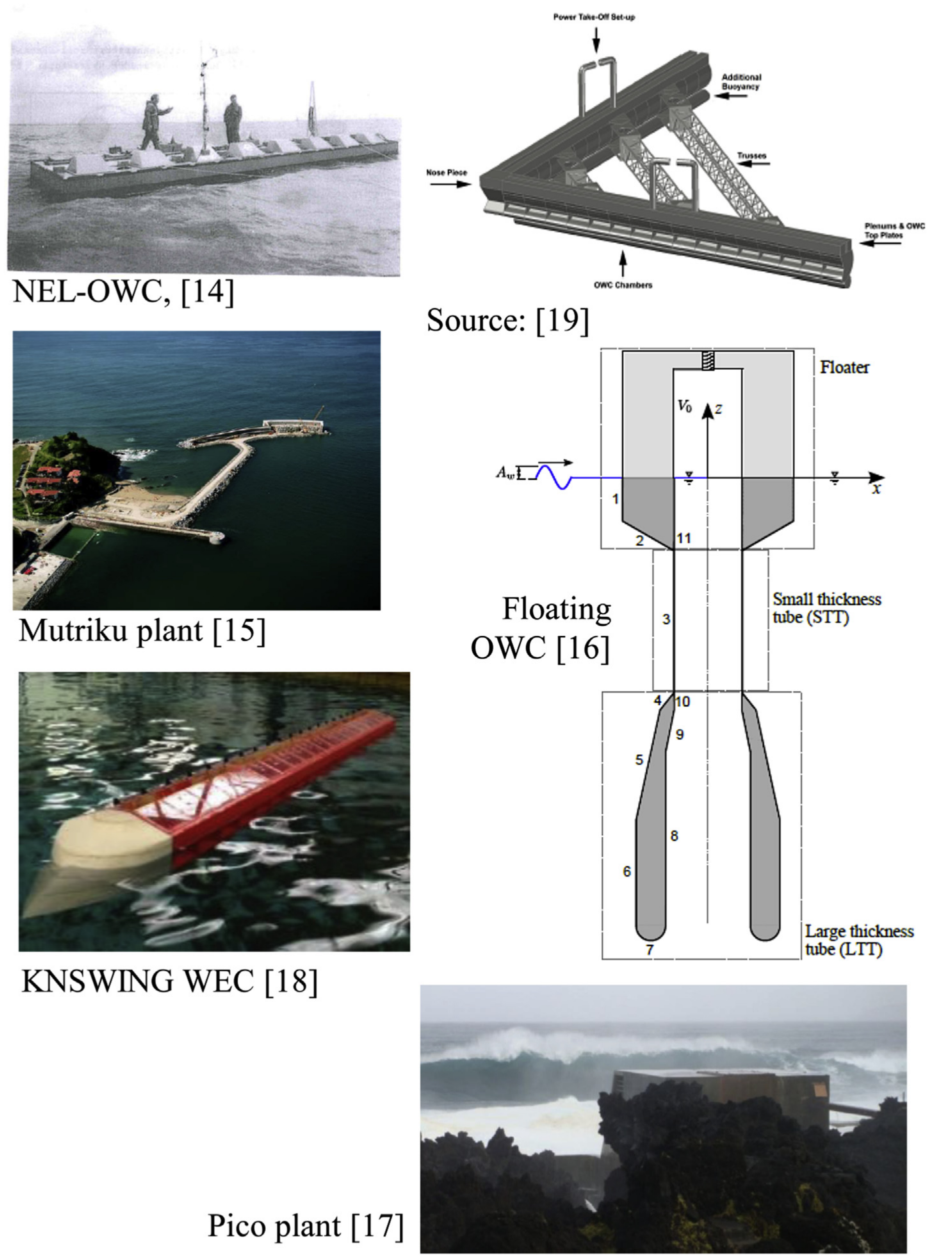

Fig. 4. Pictures of the OWC technologies covered by the sources reviewed in Section 3.1.1.

Power performance results for other OWC wave energy converters can be found in Refs. [9–11]. These sources are discussed in Section 3.1.6.

3.1.2. *Overtopping devices*

Pictures of the overtopping devices discussed in this section are shown in Fig. 5.

- Ref. [20] deals with the SSG (Sea Slot-Cone Generator) wave energy converter, an overtopping device in which the overtopping water is stored in different basins depending on the wave height. As part of plans to install a 10 m wide pilot plant in Norway, power performance was investigated through experiments on a 1/60 scale model. The mean annual energy production is estimated to be 320 MWh/y for the Norwegian site where the wave resource is 19.5 kW/m. According to Table 1 of source [20], the turbine efficiency is in the order of 85% and the generator efficiency is 96%. Thus, the mean absorber power is 45 kW/m and the CWR is 23%. This device differs from the archetypal overtopping device in Fig. 3 because it has multiple water reservoirs on top of each other. Thus, it was included in the database as a variant of an overtopping device.
- Ref. [21] presents power performance results for the well-known Wavedragon device. Experimental results from sea trials of a scale model at a benign site in Nissum Bredning in Denmark were used in conjunction with numerical models to derive non-dimensional performance of the device. Mean annual CWR was reported to be 27% for a site with wave resource 6 kW/m and device width 65 m, and 18% for a site with wave resource 24 kW/m and device width 97 m.

Power performance results for other overtopping devices can be found in Refs. [9] and [10]. These sources are discussed in Section 3.1.6.

Sea Slot-Cone Generator (SSG) [20]

Wavedragon [21]

Fig. 5. Pictures of the overtopping devices covered by the sources reviewed in Section 3.1.2.

3.1.3. Heaving devices

Pictures of the heaving devices discussed in this section are shown in Fig. 6.

- Ref. [22] deals with a heaving device. Inspired by the SEACAP technology developed by the Hydrocap company, the device has the form of a torus sliding along the mast of an offshore wind turbine. Mean annual power absorption was calculated for the Yeu site. Several diameters and drafts were considered for the torus, with and without latching control. For reasons explained in Section 2, we retained only those results with passive control in the database. Mean CWR, calculated using data from Table 2 of the paper, ranges from 3 to 9 % with diameters ranging from 11 to 20 m. This is significantly smaller than the usual mean CWR for devices of that size and operational principle. This may be explained by the fact that the PTO damping coefficient was optimized in order to maximize the power absorption in regular waves for the resonance frequency, not in order to maximize the annual energy absorption with irregular waves.
- Ref. [23] presents power performance results obtained using numerical modelling for a heaving device. The WEC is a vertical cylinder with 10 m diameter and 2 m height. It is a simplified version of the OPT technology developed in the US. The PTO damping coefficient was optimized for each sea state. The mean annual absorbed power for year 2010 was estimated to be 77 kW for a site offshore Oregon in the US, where the wave resource was 40 kW/m for that year. The mean annual CWR is 19%.
- Ref. [24] presents experimental results conducted in Denmark for the DEXA WEC. As explained in Section 2.3, it may be classified as a variant of a heaving device. A 1/30 scale model was used, with length 2.1 m and width 0.81 m. Power performance results are shown in figure 13 of the paper. Using this data and the wave scatter diagram for Yeu (having wave resource 26 kW/m), the mean annual CWR has been estimated by us to be 8% with a characteristic diameter of 22 m. The characteristic diameter was calculated according to equation (4).
- Ref. [25] presents power performance results for the Norwegian WEC technology Lifesaver, a heaving device. A prototype was installed in 2012 in the UK. The buoy is a torus with outer diameter 16 m and inner diameter 10 m. The paper reports on the experience gathered after one year of full scale sea trials. It also shows the electrical power matrix predicted by the numerical model of the device (Table 2). According to the paper, the PTO efficiency is 80%. Using equation (4), we calculated the characteristic diameter of the device to be 12.5 m. Hence, we calculated the mean annual CWR to be 12% for the 26 kW/m Yeu site.
- Ref. [26] presents numerical results for the power performance of a WEC inspired by the Wavestar WEC. It is composed of eight heaving buoys connected to a central fixed platform. Power matrices are determined for various diameters of the heaving buoys. Then, annual mean CWR is calculated for coastal locations all over the world. In Table 2 of the paper, the average mean annual CWR is reported to be 10% for 4 m diameter configuration and 15% for 15 m diameter configuration.
- Ref. [27] is the final report of a technico-economical study for four marine renewable energy technologies: three current turbines and one WEC (RM3). It is a heaving WEC, inspired by the OPT technology. The power matrix was determined using numerical modelling and electricity production calculated for a site offshore California. The wave resource is 34 kW/m. The numerical model was validated against experiments. Electricity production is 700 MWh at this site, assuming 80% PTO efficiency, 95% availability and 98% efficiency in the transmission line. Thus, the mean absorbed power is 108 kW. The diameter of the buoy is 20 m, thus the mean annual CWR is 16%.

Power performance results for other heaving devices can be found in Refs. [9–11,45]. These sources are discussed in Section 3.1.6.

3.1.4. Fixed OWSCs

Pictures of the fixed OWSCs discussed in this section are shown in Fig. 7.

- Ref. [28] is the final report of a study of the response and performance of Salter's duck. The device reacts against a fixed reference. It has three degrees of freedom: surge, heave and pitch. It extracts energy from the pitch motion only. It is classified as a variant of fixed OWSC. The report deals with numerical and experimental modelling. Both optimal reactive control and four-term control were implemented, of which only the latter is currently feasible in practice. However, even the four-term control is reactive. Indeed, in figure 5.4 of the report, it can be seen that one of the terms in the four-term control corresponds to a negative spring in pitch. For reasons explained in Section 2.2, only CWR for devices with passive control are taken into account in the database. Thus, this reference is not included. However, using power performance results with the four-term control, i.e. graph 4 in figure 6.2 of the report, and according to the methodology explained in Section 2, mean CWR estimates for the device were calculated by us, and are provided for information. They are respectively 65%, 75%, 79%, 68% for a 16, 23, 27, 38 kW/m wave resource, the device width being 30 m.
- Ref. [29] reports experimental results for top-hinged flaps. Three water depths were considered: 10, 15 and 22 m. The paper shows results for the CWR in regular and irregular waves (see

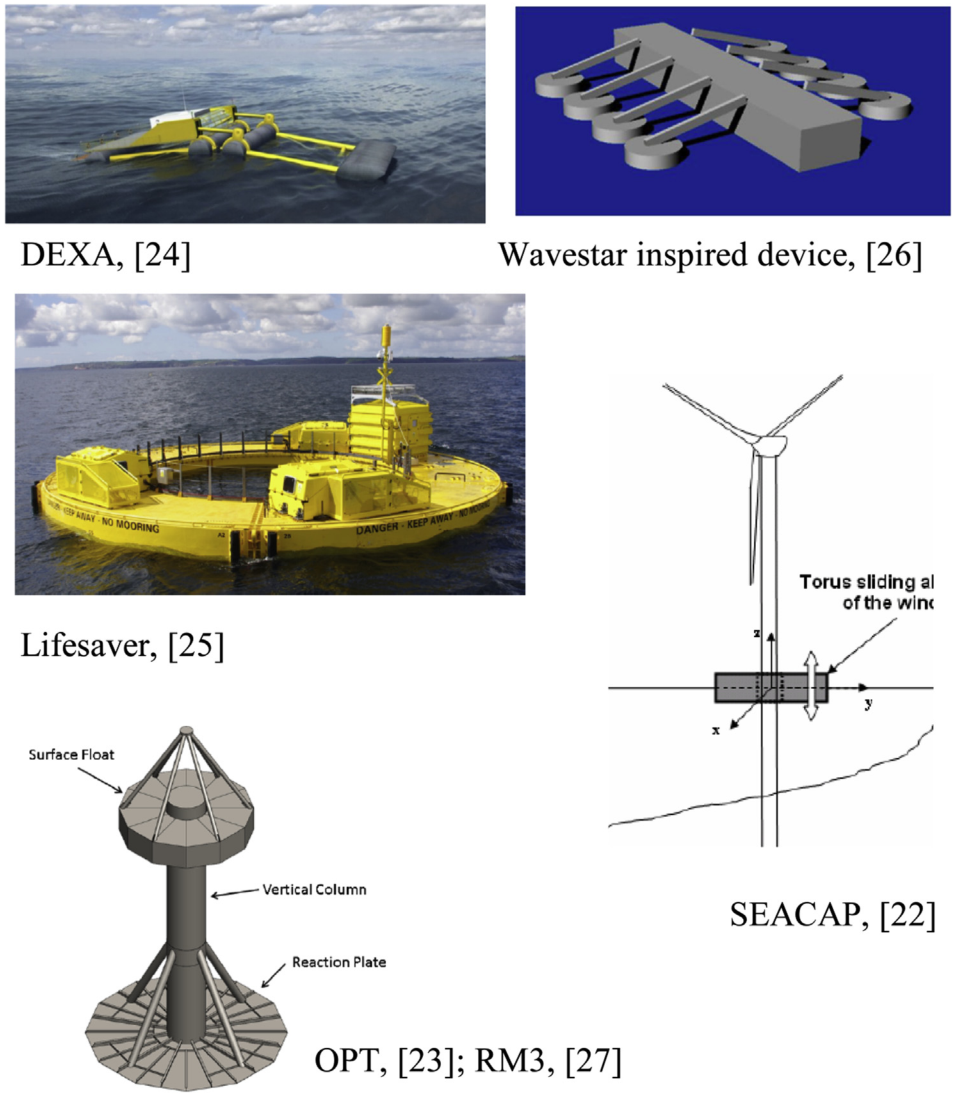

Fig. 6. Pictures of the heaving device technologies covered by the sources reviewed in Section 3.1.3.

figures 8 and 9 in the paper). It should be noted that the characteristic dimension in the paper was the cube root of the device volume. Best performance was observed for the smallest water depth, so this was retained in the database. Using data shown in figure 8 of the paper, we calculated the mean annual CWR for a site close to Yeu island offshore the French Atlantic coast, according to the methodology explained in Section 2. The wave resource is 25 kW/m, the CWR 25%, and the width 12 m. The flaps being top-hinged, they are classified as a variant of fixed OWSC.

- Ref. [30] reports on experiments conducted on the Biopower technology in Australia. It is classified as a variant of fixed OWSC because it uses a vertical cylinder instead of a vertical flap. The technology was tested experimentally with various ballast configurations in sixteen different random sea states. The first half of the sea states are representative of winter conditions at the EMEC test site, and the other half of summer conditions. Probabilities of occurence of these sea states at EMEC are given in the paper in Table 1, allowing calculation of the wave resource in summer and winter conditions: 10 and 67 kW/m, respectively. Table 4 in the paper shows power performance for the summer and winter seasons for each configuration tested, with configuration 5 retained by us as the one with the best performance, namely 41 kW in summer and 130 kW in winter. The device width being 6.6 m, the mean CWR is thus 45%.
- Ref. [31] reports power performance for a fixed OWSC in shallow water depth. Figure 7 of the paper shows results of mean CWR derived from experiments conducted in a wave tank at Queen's University Belfast in Northern Ireland. Mean CWR is 35% for the 6 m width device, increasing with width up to 65% for a 24 m wide device. The wave scatter diagram used to calculate the mean CWR is not given in the paper.
- Refs. [32–34] present results of experiments of the WEPTOS technology. The WEPTOS is composed of a V-shaped platform and WECs similar to Salter's ducks. The ducks are mounted on a common spine on each branch of the V. They are classified as variant of the fixed OWSC. A scale model was tested in 2011 in Spain and the performance of the machine was measured in random waves, as well as bending moments in the structure and mooring forces. Building on experimental results, prototype performance at a scaling ratio of 1/15 was predicted in Ref. [32] at the Hanstholm site in Denmark where the wave resource is 6 kW/m. The mean annual CWR is thus expected to be 12% with a WEC width of 3.6 m. Using the same experimental data,

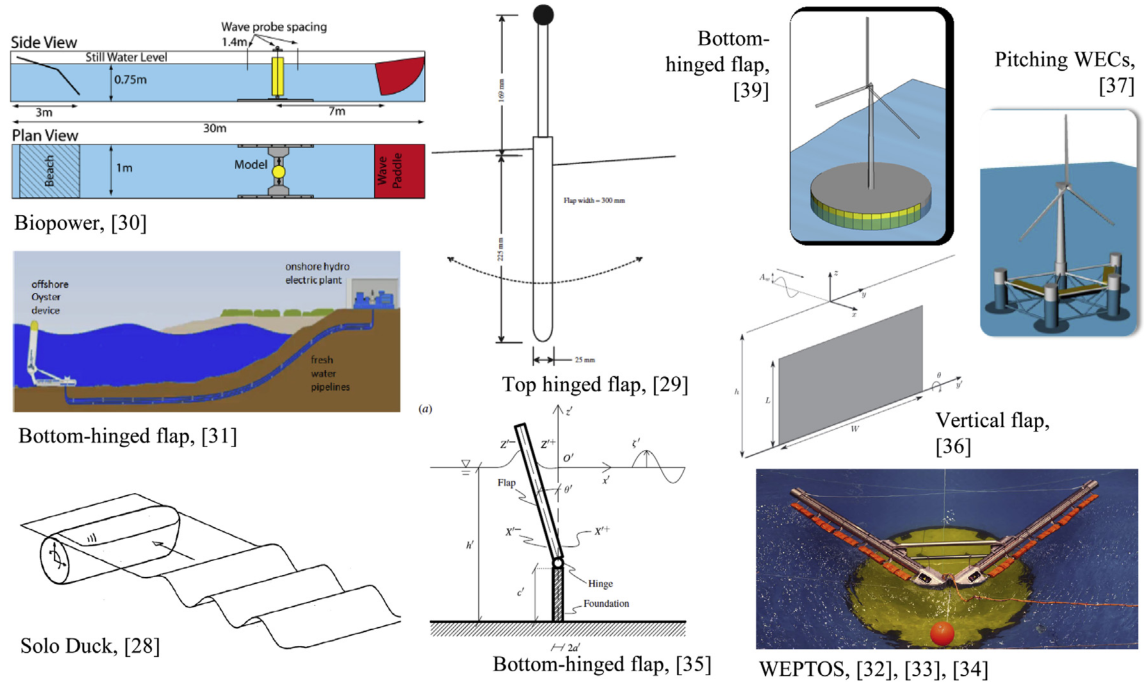

Fig. 7. Pictures of the fixed OWSCs covered by the sources reviewed in Section 3.1.4.

prototype performance at scaling ratios of 1/12, 1/15, 1/20 and 1/25 is predicted in Ref. [33] at the Hanstholm site (Table 2 of Ref. [33]) and at site in the Danish North Sea where the wave resource is 16 kW/m (Table 3 of Ref. [33]). In Table 2 of source [34], mean annual power production is reported for two other sites in Denmark, one site in France and the EMEC test site in Scotland. 90% PTO efficiency and 98% availability was used in Ref. [34] according to private communication with the authors.

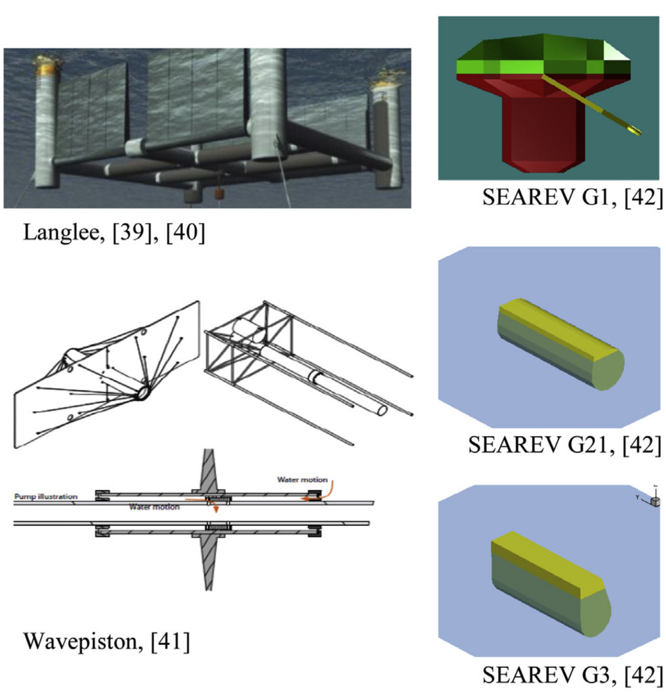

Fig. 8. Pictures of the floating OWSCs covered by the sources reviewed in Section 3.1.5.

The performance results from Refs. [32–34] are summarized in Table 1.

- Ref. [35] is a mathematical and numerical study of a fixed OSWC in a canal. The problem is equivalent to an infinite line array of devices facing the incident waves. The device is inspired by the Aquamarine/Oyster. Figure 8 in the paper shows CWR for three device widths. The canal width is fixed at 91.6 m. According to the method described in Section 2, we calculated the mean actual CWR for the Yeu site, having 26 kW/m wave resource, to be 22% for the 6 m wide device, 40% for the 12 m device and 55% for the 18 m device.
- Ref. [36] presents numerical results for the power performance of a combined wind and wave energy platform. It is composed of a large floating barge with twenty vertical flaps on its wave facing side and a 5 MW wind turbine mounted on top of it. The floating barge is large and stable, thus the WECs can be classified as a variant of fixed OWSCs. The power matrix was determined using numerical modelling. Table 4 of the paper shows that the hydrodynamic efficiency is 72% for a 26 kW/m site using the barge diameter (100 m) as the reference width. Using the WEC width (10 times 16 m), the mean annual CWR is calculated to be 45%.
- Ref. [37] shows numerical results for the power performance of a combined wind and wave energy platform. It is composed of a semi-submersible platform with a 5 MW wind turbine mounted on top of it. Twelve pitching WECs are installed on the wave facing braces of the platform. The width of the WECs is 9 m. Based on the geometry of the WECs, they are classified as a variant of fixed OWSC. The power matrix was determined using numerical modelling. Table 4 of the paper shows that the mean annual CWR hydrodynamic efficiency is 61% for a 26 kW/m site.
- Ref. [38] presents numerical results for the power performance of submerged and surface piercing bottom-hinged plate wave energy converters. The devices are inspired by the Aquamarine/Oyster and the AW-Energy/WaveRoller. Influence of the flap height to water depth ratio and flap width to water depth ratio are investigated. Figure 14 in the paper shows CWR for a surface

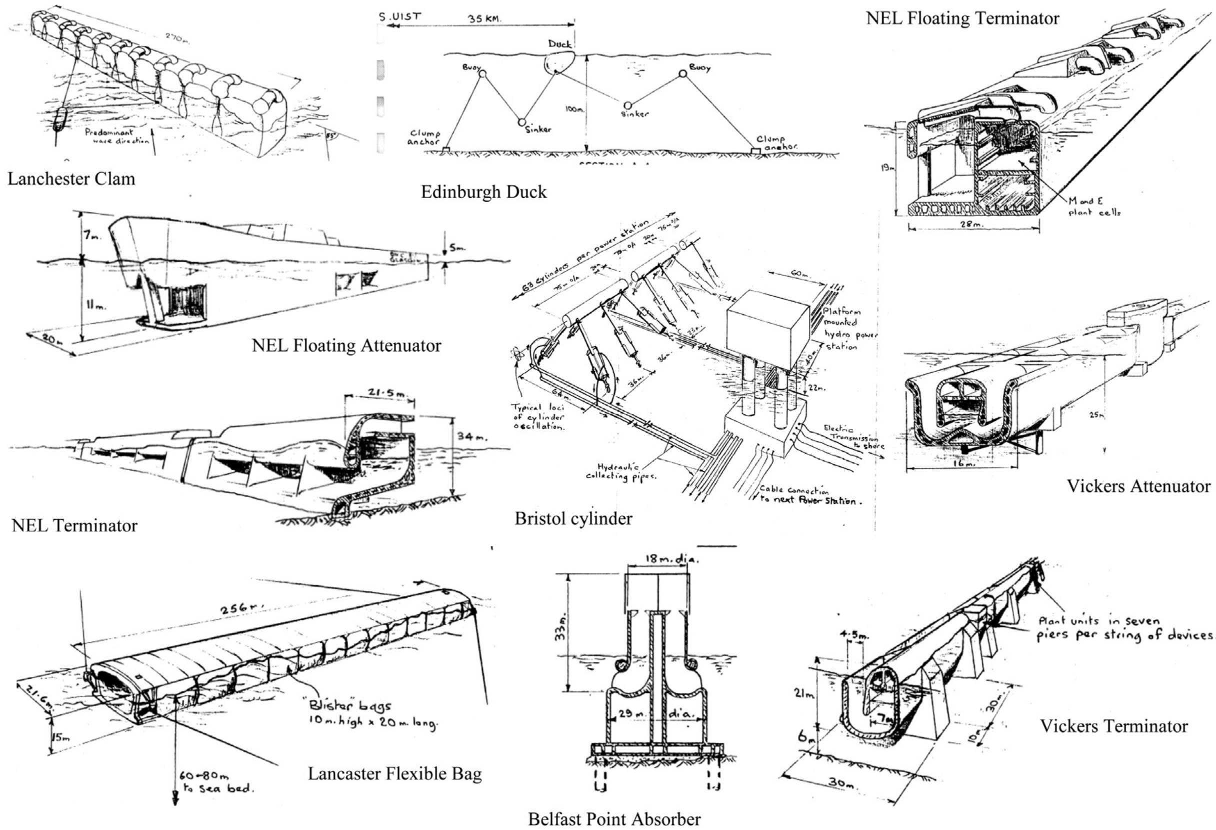

Fig. 9. Pictures of wave energy converters investigated in Ref. [43].

piercing flap in irregular waves (with Pierson-Moskowitz spectrum) for five flap widths. Figure 19 in the same paper shows CWR for a 20 m wide flap for five flap heighths. The water depth is 10 m. According to the method described in Section 2, we calculated the mean actual CWR for the Yeu site. Best performance was observed for the surface piercing flap, so this was retained in the database (the reference highlights the importance of having a surface-piercing device for the maximization

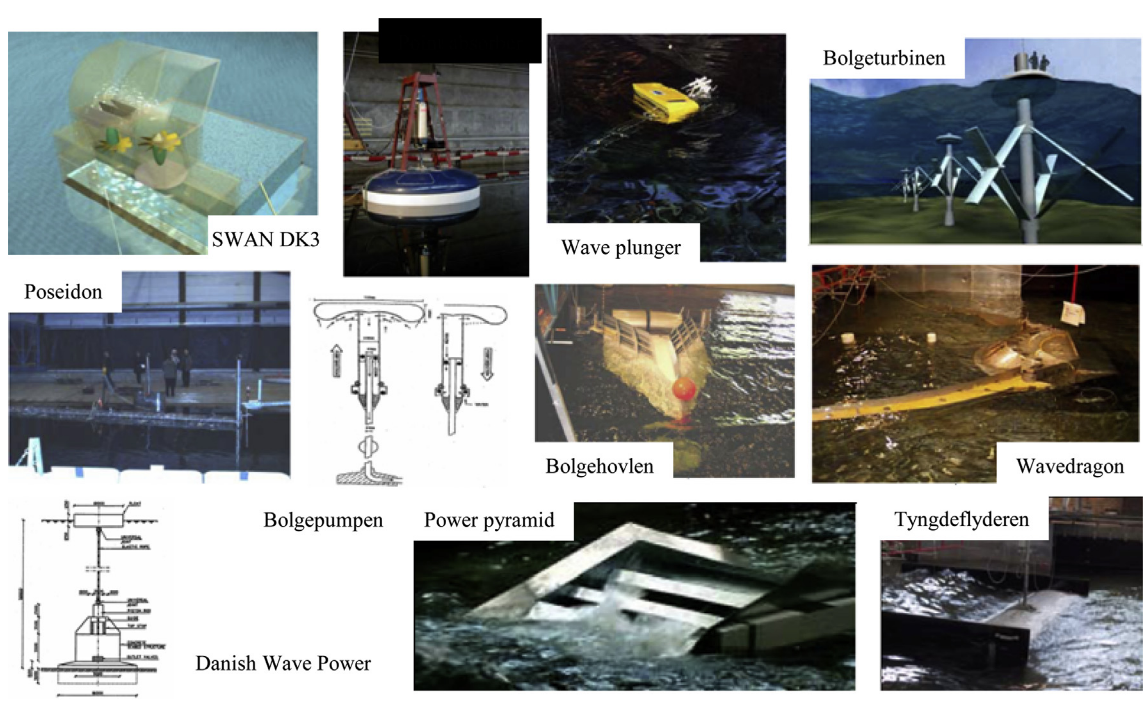

Fig. 10. Pictures of wave energy converters investigated in Ref. [9].

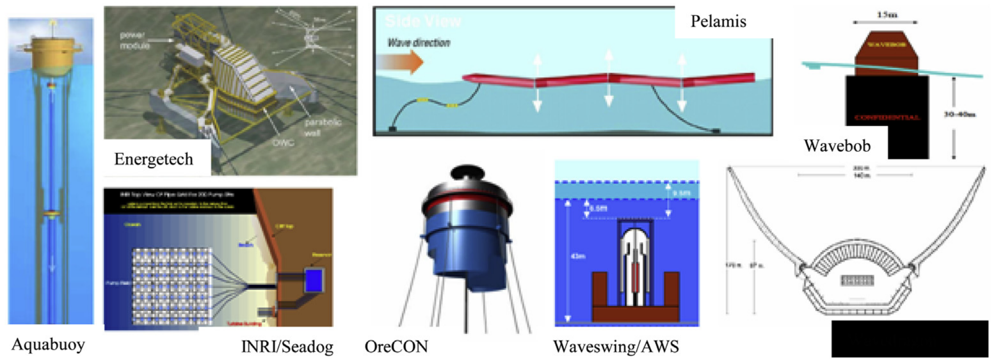

Fig. 11. Pictures of wave energy converters investigated in Ref. [10].

of the wave energy absorption for OWSCs). The CWR estimates are 17, 36, 72 and 64% for flap widths of respectively 5, 10, 20 and 50 m and for a 26 kW/m site.

Power performance results for other OWSCs can be found in Refs. [11,44,45]. These sources are discussed in Section 3.1.6.

3.1.5. *Floating OWSCs*

Pictures of the floating OWSCs discussed in this section are shown in Fig. 8.

- Refs. [39] and [40] reports on experiments conducted on the Langlee technology, consisting of oscillating flaps mounted on a floating structure. Experiments were conducted at Aalborg University in Denmark. Experiments carried out at small scale in order to determine the power performance of these devices in five random sea states with significant height ranging from one to five metres. Mean annual CWR were obtained by weighting power performance for each sea state with its probability of occurence at a site offshore Denmark. The mean annual resource was 16 kW/m Table 6 of source [39] shows that the mean CWR was found to be 7% for a device width 25 m and 9% for devices width 37.5 m and 50 m. Note that the total flap width has been taken into account in the CWR. Ref. [40] reports on a second round of experiments conducted on the same technology. The tested geometry differed from Ref. [39]in that: surface piercing flaps were used. This was found to increase efficiency compared to a fully submerged flap configuration. Buoyancy of the flaps was also found to have a large impact on efficiency. Tables 3 and 4 of Ref. [40] show the estimates of yearly power production for several scales of the device (1/20, 1/40, 1/60) and two locations. For the Danish North Sea site, whose wave resource is 16 kW/m, yearly power production is 620 MWh/y for a device width 25 m. For the Runde site, whose wave resource is 21 kW/m, yearly power production is respectively 420 MWh/y, 1870 MWh/y and 3720 MWh/y for devices width 25 m, 50 m and 100 m. The total width of flaps for the device being twice the device width, the CWR is 9% for the site with 16 kW/m resource: for the site with 21 kW/m resource, the CWR is respectively 5%, 10% and 10% for devices width 25 m, 50 m and 100 m.
- Ref. [41] reports on experiments in Denmark using the Wave-piston technology. This device is made of vertical plates facing the waves and sliding along one long common axis, and can be classified as a variant of floating OWSC. As for Refs. [9] and [39], the device was tested for five representative sea states. The mean CWR was obtained by weighting performance results by their probabilities, and mean CWR is 8% for a 15 m wide device (see Table 3 of the paper) and a wave resource of 12 kW/m. Another site offshore Italy was also considered, for which mean CWR is 15% for a wave resource of 3.5 kW/m.

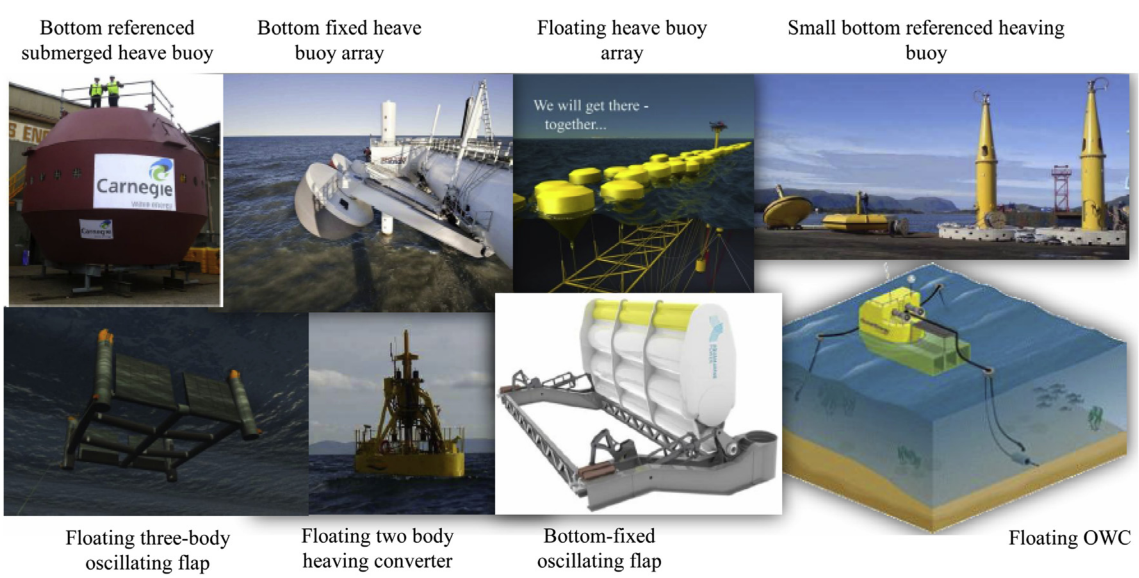

Fig. 12. Pictures of wave energy converters investigated in Ref. [11].

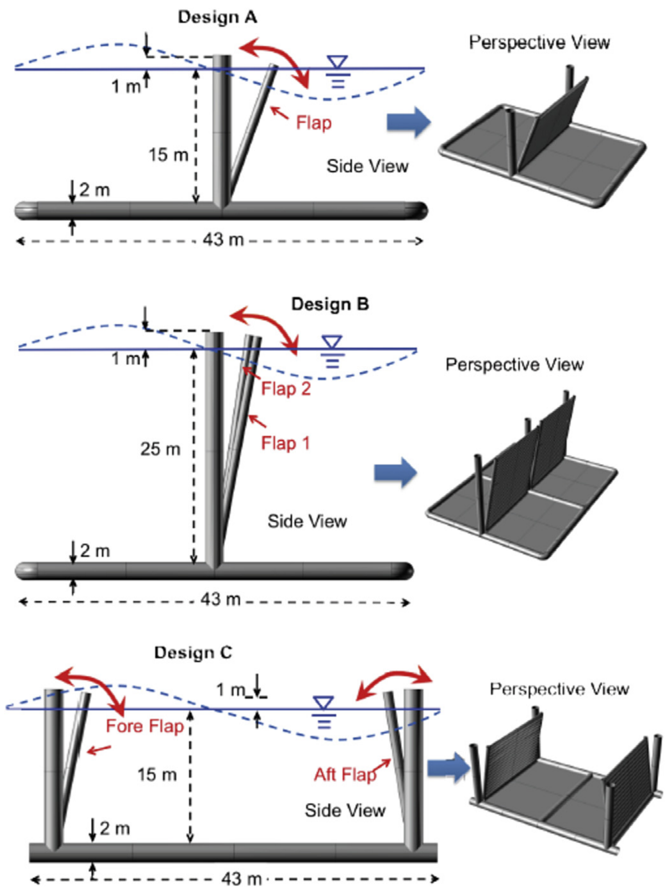

Fig. 13. Pictures of wave energy converters investigated in Ref. [44].

- Ref. [42] deals with the development of the SEAREV WEC technology. The SEAREV device absorbs wave power through pitch motion; as such, it can be classified as a variant of floating OWSC. Mean annual absorbed power with and without control was derived using numerical modelling. In the database, we retained only results with passive control. Three versions of the SEAREV technology are presented in the source [42]. They are labelled SEAREV G1, SEAREV G21 and SEAREV G3. The width of SEAREV G1 is 13.6 m, whereas it is 30 m for SEAREV G21 and SEAREV G3. According to data shown in Tables 1, 2 and 5 of Ref. [42], the mean CWR are respectively 20%, 16% and 25% for SEAREV G1, SEAREV G21 and SEAREV G3 for a site with 25 kW/m resource.

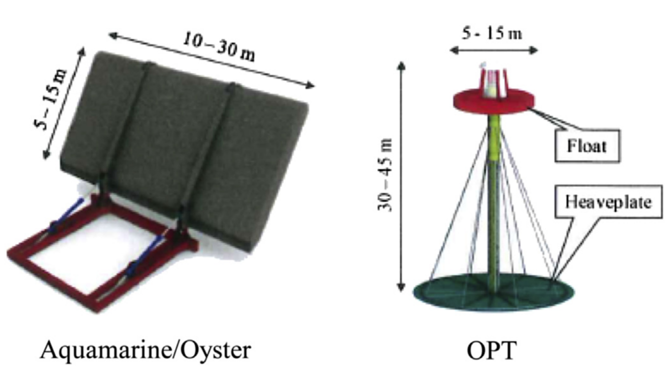

Fig. 14. Pictures of wave energy converters investigated in Ref. [45].

Power performance results for other floating OWSCs can be found in Refs. [11] and [44]. These sources are discussed in Section 3.1.6.

3.1.6. Sources considering technologies with various working principles

- Ref. [43] is a report presenting results of a technical-economical assessment of ten wave energy converters which were developed in the UK in the late 70s and early 80s. Six of the devices are OWCs or variants of OWCs, the others being variants of fixed OWSCs, including the famous Edinburgh Duck and Bristol Cylinder. The devices are depicted in Fig. 9. Power performance was assessed using experiments in directional random waves, except in the case of the NEL Terminator device, for which numerical models were used. Scale models of the devices were tested for 46 sea states representative of the South Uist offshore site in the UK. Mean annual CWR for each technology are shown in device data sheets in Section 5 of source [43], and recalled in Table 2. It may be observed that power performance for the Vicker's terminator, the Vicker's Attenuator and the Lancaster Flexible Bag is significantly lower than for other devices with same operational principle and comparable dimensions. According to Ref. [43], this is due to the use of manifolding in the PTO.
- Ref. [9] is the final report of a research program conducted in Denmark from 1997 to 2002. The aim of the program was to investigate a large number of WEC technologies. Twelve devices were considered: one floating OWC, several wave activated bodies, several overtopping devices and one wave turbine. The devices are depicted in Fig. 10. Experiments were conducted at small scale in order to determine the power performance of these devices in five random sea states with significant height ranging from one to five metres. Mean annual CWR were obtained by weighting power performance for each sea state with its probability of occurence at a site offshore Denmark. The scatter diagram resulted from Ref. [56]. The mean annual resource was 16 kW/m. Mean annual CWR η_1 for each technology, directly taken from Table 8.6 of source [9], is recalled in Table 3. Note that for some cases, a few designs of the same technology were tested: in these cases, we retained only that with best performance. For heaving devices, we calculated the dimension using equation (4).
- Ref. [10] is a report presenting results from a study conducted by E2I EPRI on the technico-economical feasibility of wave energy conversion in the US in 2004. Eight technologies were assessed: Ocean Power Delivery (currently Pelamis Wave)/Pelamis, Energetech, Wavedragon, Waveswing/AWS, Wavebob, Aquaenergy/AquaBuOY, OreCON and INRI/SEADOG. The devices are depicted in Fig. 11. Power production calculations were based on data and a power matrix provided by the technology developers. Results have been extracted from the report and summarized in Table 4.
- Ref. [11] presents the results of a numerical benchmarking study of a selection of eight wave energy technologies inspired by devices which are or were being developed. The selection includes a floating OWC, several heaving devices, one floating OWSC and one fixed OWSC. The devices are shown in Fig. 12. The study used numerical modelling: Wave to Wire (W2W) models were developed and used to derive the power matrix of each technology. Then, the mean annual power absorption was calculated at five European possible deployment locations whose wave resource ranges from 15 to 80 kW/m. Depending on the technology, it was shown that the mean CWR may depend significantly on the resource, up to a factor of three. However, the lowest mean CWR was always obtained for the most energetic site (80 kW/m at Belmullet, Ireland). As this is much higher

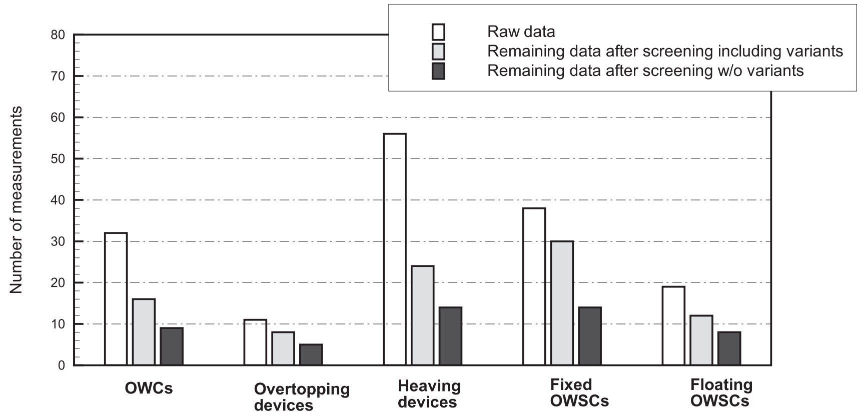

Fig. 15. Number of measurements per category of WECs.

than the usual global figures for wave resource (10–40 kW/m, see Ref. [58]), we did not take it into account. Table 5 summarizes mean CWR for the eight technologies extracted from figures 12–19 of Ref. [11].

- [44] presents numerical results for the power performance of fixed and floating OWSCs. Three configurations are considered: (A) one flap mounted on a supporting frame, (B) two flaps that sit side by side and (C) two flaps, one in the front and one in the back. The devices are depicted in Fig. 13. In all configurations, the flap width is 25 m. Numerical modelling was used to derive power matrices for each configuration and for different mooring configurations (fixed supporting frame, taut mooring and slack mooring). With the fixed supporting frame, the devices are classified as variants of fixed OWSC because the flap height is not close to the water depth. The wave scatter diagram is shown in Table 4. The wave resource is 30 kW/m. Annual average electrical power is shown in figure 7 of the paper. 80% PTO efficiency is assumed as well as 95% availability and 98% efficiency in the transmission line. Table 6 shows the mean annual absorbed power and CWR for the configurations considered in the paper.
- [45] presents numerical results for the power performance of a two-body heaving device and a fixed OWSC. The devices are shown in Fig. 14. The heaving device is 15 m wide. On page 99 of source [45], it is reported that the average electric power is 82 kW, with hydraulic PTO efficiency of 72%. The wave resource at the site being 31 kW/m, the mean annual CWR is 25%. For the fixed OWSC, the width is 25.5 m. It is reported (page 108 of source [45] that the average electric power is 170 kW with hydraulic PTO efficiency of 75%. The wave resource at the site being 18 kW/m, the mean annual CWR is 49%.

3.2. Summary table

The data collected for mean annual CWR is synthesized in Tables 7–9. The WECs have been grouped in ten categories as discussed in Section 2.3: OWCs and variants, overtopping devices and variants, heaving devices and variants, fixed OWSC and variants, floating OWSC and variants. Devices not belonging to any of these categories were not included in the tables. In these, the devices are labelled by their commercial names when available, or by the description of their operational principle. CWR is reported alongside the corresponding wave resource for which it was measured and the dimension on which the CWR was built.

Where available, information relating to how the CWR was obtained (model tests, numerical modelling or measurements on full scale prototype) is also reported. In more than half of the cases, CWR were obtained through experiments at model scale or prototype scale.

The tables also indicate whether the source is independent from the technology developer. 'Developer' indicates that the information comes from the technology developer itself whereas 'independent' means that the CWR was established by an independent body (usually a research lab).

4. Discussion

In total, 156 measurements of CWR were collected. Fig. 15 shows the distribution of measurements as a function of the WEC categories. The category for which the most performance information was found (56 measurements) was heaving devices, followed by fixed OWSCs and OWCs. This is somewhat surprising, as OWCs have been studied for more than 30 years, whereas fixed OWSCs have only started developing over the last decade. The least information was found for floating OWSCs and overtopping devices.

Some of the measurements are believed to be unreliable (lines in italics in Tables 7 and 8). Indeed, for the AWS and the ORECON/MR1000, the CWR is five to ten times larger than other similar technologies. Because the available source information does not provide an explanation for these discrepancies, these measurements were discarded from further analysis. The Hydrocap/SEACAP device was also discarded because it is five times smaller than device of similar dimensions, and because as explained before, the performance is small because the PTO damping coefficient was optimized for the resonant period in regular waves, and not for the mean annual power absorption in irregular waves.

Moreover, for some of the technologies, CWR is available for several levels of wave resource. The CWR for the level of wave resource closest to 25 kW/m was selected as the most representative [58].

After screening, 90 measurements were retained for further analysis. The two categories with the most measurements in the screened data, including variants, are fixed OWSCs and heaving

Table 10
Mean and standard deviation of CWR and characteristic dimension for each WEC category.

		OWCs	Overtopping devices	Heaving devices	Fixed OWSCs	Floating OWSCs
Capture width ratio (%)	Mean	29	17	16	37	12
	STD	13	8	10	20	5
Characteristic dimension (m)	Mean	20	124	12	18	33
	STD	10	107	7	14	24

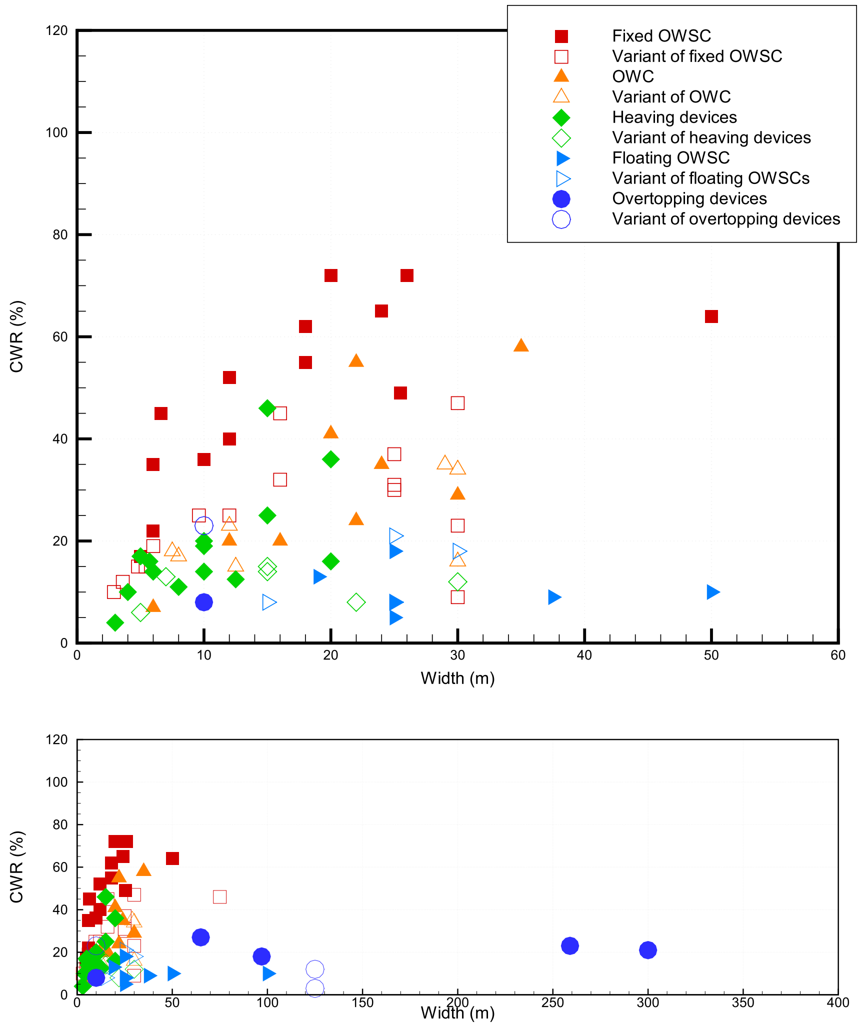

Fig. 16. CWR as a function of the WEC characteristic dimension and the WEC category. Top figure zooms in on the subdomain [0,60] m part of the bottom figure.

devices, with 30 and 24 measurements respectively. OWCs, floating OWSCs and overtopping devices had 16, 12 and 8 measurements, respectively. Excluding variants, the categories with most measurements are heaving devices and fixed OWSCs, both with 14 measurements. OWCs, floating OWSCs and overtopping devices had 9, 8 and 5 measurements, respectively.

Statistical analysis was performed. For each category, Table 10 shows the mean and the standard deviation for both the CWR and the characteristic dimension of the WECs. Variants were taken into account. According to the mean, the most efficient category of WECs is fixed OWSCs with a mean CWR of 37%. The second most efficient WECs are OWCs (mean CWR of 29%), followed by overtopping devices (17%), heaving devices (16%) and floating OWSCs (12%).

One can see that standard deviations of the CWR are large - typically, half of the mean CWR. This shows that, within a given category, the power performance of devices can differ widely. However, the mean CWR gives a good indication of the typical order of magnitude of the power performance of each of these categories.

From Table 10, it can also be seen that heaving devices are typically the smallest WECs (having mean characteristic dimension 12 m). The second smallest are the fixed OWSCs (18 m) and the OWCs (20 m), followed by the floating OWSCs (33 m) and the large overtopping devices (124 m).

Fig. 16 shows the CWR as a function of the WEC characteristic dimension and the WEC category. Although the level of scattering is large, trends can be identified:

- Floating OWSCs and overtopping devices appear to be the least efficient devices, in terms of absorbing wave energy.
- Fixed OWSCs appear to be the most efficient devices.
- Heaving devices and OWCs appear to be in the middle of the efficiency range.

Being able to identify these trends from the data gives confidence in the classification that has been used (OWCs, overtopping

Table 11
Best fit equations and 95% confidence interval for each WEC category.

	Best fit	95% Confidence interval
OWCs	$\tilde{\eta}_1 = 1.4B + 2.1, \quad B \in [0, 40]$	$\tilde{\eta}_1 \pm 30\sqrt{1.1 + \frac{(B-21)^2}{81}}$
Overtopping devices	$\tilde{\eta}_1 = 0.026B + 15.6, \quad B \in [0, 320]$	$\tilde{\eta}_1 \pm 26\sqrt{1.2 + \frac{(B-146)^2}{7230}}$
Heaving devices	$\tilde{\eta}_1 = 1.3B + 5.6, \quad B \in [0, 20]$	$\tilde{\eta}_1 \pm 21\sqrt{1.1 + \frac{(B-10)^2}{31}}$
Fixed OWSCs	$\tilde{\eta}_1 = 1.9B + 20.5, \quad B \in [0, 20]$	$\tilde{\eta}_1 \pm 25\sqrt{1.1 + \frac{(B-15)^2}{61}}$
Floating OWSCs	$\tilde{\eta}_1 = 8.5, \quad B \in [0, 100]$	$\tilde{\eta}_1 \pm 12\sqrt{1.1 + \frac{(B-53)^2}{1090}}$

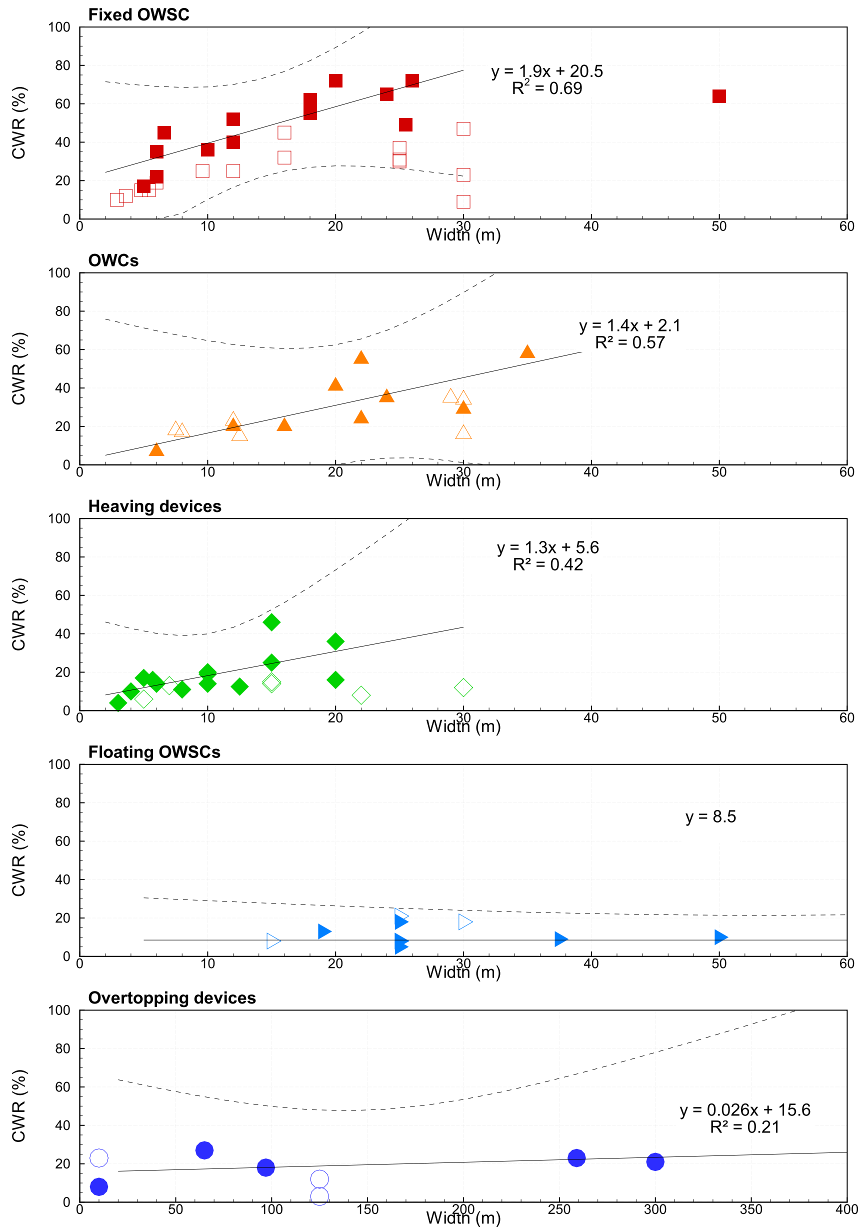

Fig. 17. Data points, best fit equations and 95% confidence interval for each category of WECs. For each category, empty symbols are for devices which are variants of the archetypal realization.

devices, heaving devices, fixed and floating OWSCs). It indicates that the classification reflects rather well the underlying physical principles that lead to wave energy absorption by these WEC technologies.

It can be seen from Fig. 16 that CWR increases with the characteristic dimension for OWCs, heaving devices, overtopping devices and fixed OWSCs. Linear regression was performed for these categories on the most representative measurements points (i.e variants were not taken into account).

It yields a reasonable fit for the OWCs and the heaving devices, the coefficient of determination being 0.57 for the OWCs and 0.42 for the heaving devices. For overtopping devices, the linear fit is only approximate, the coefficient of determination being 0.21. This is due to the limited number of measurement points and an outlier having high CWR (27%) for the width of 65 m. One may note that the wave resource corresponding to this measurement point is much smaller (6 kW/m) than for the other measurement points (in the order of 20 kW/m, see Table 7). It may be expected that the same device at a site with larger wave resource has a smaller CWR, thus more in agreement with the linear fit.

For fixed OWSCs, it can be observed in 16 that CWR increases with width for widths between 0 up to 30 m. In the database 9, it can be seen that several devices in this category have a CWR greater than 50% for widths in the order of 20–30 m. On the other hand, it is well known from Ref. [50] that the maximum CWR is 50% for devices whose width is greater than the wavelength. Consequently, the increase in CWR with width that can be seen in Fig. 16 for fixed OWSCs must be valid only for small widths. When further increasing the width, the CWR must reach a maximum and then decrease below 50% for long devices. This is in agreement with the outlier with width 50 m, whose CWR is smaller than similar devices with half its width. Thus, linear fit was performed only on measurements points with width less than 30 m for fixed OWSCs. It yields a reasonable fit, the coefficient of determination being 0.69.

For floating OWSCs, there is no clear relationship between the CWR and the characteristic dimension. For these categories, the best fit appears to be the mean value of the data.

For each category, Table 11 shows the best fit equations and the 95% confidence interval, calculated according to [57]. Fig. 17 shows, for each category, the data points, the best fit equations and the 95% confidence interval. One can see that all data points are covered by the confidence interval. For each category, devices which are variants of the operational principle have also been plotted (empty symbols). Again, all these points except one are covered by the confidence interval. This gives confidence in the classification choices that have been made in this work.

Conversely, the results from the statistical analysis (Table 11) may be used to estimate the typical power performance for a given category of WEC, a characteristic dimension B and a for given mean wave resource J using:

$$P = \tilde{\eta}_1 BJ \tag{5}$$

This may be useful in the early stages of WEC design, in order to check whether power performance of a particular WEC is in the range of performance figures available in the literature. It may help in detecting mistakes in the early stage of modelling, for instance, and may also be used in technico-economical prospective studies in order to estimate the wave energy potential of typical WEC technologies. However, it should not be used to assess the actual performance of a given WEC as it may differ significantly from the typical power performance of WECs of the considered category.

5. Conclusion

In this paper, available information from the literature relating to hydrodynamic power performance of WECs has been reviewed. A database was established that contains information on the WEC category (OWCs, overtopping devices, heaving devices, fixed OWSCs, floating OWSCs), its CWR, its characteristic dimension, the wave resource, the methodology that was used to derive the performance, and the reference for the information.

Analysis of this database indicated that the least efficient categories of WECs, in terms of absorbing wave energy, are floating OWSCs and overtopping devices, the most efficient are fixed OWSCs, with heaving devices and OWCs in the middle of the efficiency range. It is important to note that here, efficiency relates to hydrodynamic power performance (energy absorption) and not economical performance (cost of energy). Efficiency in the PTO system and the power conversion chain, as well as fabrication and operation costs, may be such that the most efficient device hydrodynamically speaking can be the least efficient device from perspective of cost of energy.

Statistical analysis was performed and statistical relationships were derived relating CWR to the characteristic dimension of WECs and the WEC category. It must be noted that uncertainties are large in the statistical results, as the number of measurements is rather small. However, it is believed that this statistical work may prove to be useful both in high level prospective studies and in detecting mistakes in the early stages of modelling.

It was observed that hydrodynamic performance varies significantly depending on the WEC category. In order to further investigate the underlying reasons for this, future work may compare capture width as a function of angular frequency for typical examples of the categories. Finally, WECs not belonging to one of the five categories listed above were not considered in this study because they are relatively new concepts and would constitute a category of their own. When more information becomes available for these new technologies, it may be interesting to compare their hydrodynamic performance with those of the categories considered in this paper.

Acknowledgements

The author gratefully acknowledges the financial support of the French Institut pour la Transition Energétique (ITE) France Energies Marines through the WECEXPERT project.

References

[1] Falnes J. A review of wave energy extraction. Mar Struct 2007;20:185–201.
[2] Drew B, Plummer AR, Sahinkaya MN. A review of wave energy converter technology. Proc ImechE Part A: Journal of Power and Energy 2009;223:887–902.
[3] Sabzehgar R, Moallem M. A review of ocean wave energy conversion systems. In: Proc. of the 2009 IEEE Electrical Power & Energy Conference, Montreal, QC, Canada; 2009.
[4] Falcão A F de O. Wave energy utilization: a review of technologies. Renew Sustain Energy Rev 2010;14(3):889–918.
[5] Aubry J, Ben Ahmed H, Multon B, Babarit A, Clement AH. Wave energy converters. In: Multon, editor. Marine renewable energy handbook. Paris: Wiley-ISTE; 2011. p. 323–63.
[6] Guedes Soares C, Bhattacharjee J, Tello M, Pietra L. Review and classification of wave energy converters. In: Santos TA, et al., editors. Maritime Engineering and Technology. London: Taylor & Francis Group; 2012. p. 585–94.
[7] Lopez I, Andreu J, Ceballos S, Martinez de Alegria I, Kortabarria I. Review of wave energy technologies and the necessary power-equipment. Renew Sustain Energy Rev 2013;27:413–34.
[8] Guedes Soares C, Bhattacharjee J, Karmakar D. Overview and prospects for offshore wave and wind energy. Brodogradnja 2014;65(2):91–113.
[9] Meyer NI, McDonald Arnskov M, Vad Bennetzen LCE, Burcharth HF, Bunger J, Jacobsen V, et al. Bølgekraftprogram: Afsluttende rapport fra Energistyrelsens Rådgivende. Rambøll, Teknikerbyen 31, 2830 Virum, Denmark: Bølgekraftudval Bølgekraftudvalgets Sekretariat; 2002. In Danish.
[10] Previsic M, Bedard R, Hagerman G. E2I EPRI assessment: offshore wave energy conversion devices. E2I EPRI WP-004-US-Rev1. Electricity Innovation Institute; 2004.
[11] Babarit A, Hals J, Muliawan MJ, Kurniawan A, Moan T, Krokstad J. Numerical benchmarking study of a selection of wave energy converters. Renew Energy 2012;43:44–63 [with Corrigendum in Renewable Energy, 2015, Vol. 74, pp. 955–957].
[12] Pecher A. Performance evaluation of wave energy converters. Aalborg: Department of Civil Engineering, Aalborg University; 2012 [DCE Thesis; No. 38].
[13] Babarit A, Hals J. On the maximum and actual capture width ratio of wave energy converters. In: Proc.. of the 11th European Wave and Tidal Energy Conference, Southampton, UK; 2011.
[14] Count BM. On the hydrodynamic characteristics of wave energy absorption. In: Proc. of the 2nd International Symposium on Wave energy utilization, Trondheim, Norway; 1982. p. 155–74.
[15] Torre-Enciso Y, Ortubia I, Lopez de Aguileta LI, Marques J. Mutriku Wave Power Plant: from the thinking out to the reality. In: Proc. of the 8th European Wave and Tidal Energy Conference, Uppsala, Sweden; 2009.
[16] Gomes RPF, Henriques JCC, Gato LMC, Falcão AFO. Design of a floating oscillating water column for wave energy conversion. In: Proc. of the 9th European Wave and Tidal Energy Conference, Southampton, UK; 2011.
[17] Pecher A, Le Crom I, Kofoed JP, Neumann F, de Brito Azevedo E. Performance assessment of the Pico OWC power plant following the EquiMar methodology. In: Proc. of the 21th International Offshore and Polar Engineering Conference, Hawaii, USA; 2011.
[18] Nielsen K, Jacobsen FP, Simonsen M, Scheijgrond P. Attenuator development phase I, MARINET Infrastructure Access Report, Infrastructure: UCC-HMRC Ocean Wave Basin. User-Project: KNSWING, MARINET-TA1-KNSWING. 2013.
[19] Kelly T, Dooley T, Campbell J, Ringwood J. Comparison of the experimental and numerical results of modelling a 32-oscillating water column (OWC), V-shaped floating wave energy converters. Energies 2013;6:4045–77.
[20] Margheritini L, Vicinanza D, Frigaard P. SSG wave energy converter: design, reliability and hydraulic performance of an innovative overtopping device. Renew Energy 2009;34:1371–80.
[21] Parmeggiani S, Chozas JF, Pecher A, Friis-Madsen E, Sorensen HC, Kofoed JP. Performance assessment of the Wave Dragon wave energy converter based on the Equimar methodology. In: Proc. of the 9th European Wave and Tidal Energy Conference, Southampton, UK; 2011.
[22] Baudry V, Babarit A. Assessment of the annual energy production of a heaving wave energy converter sliding on the mast of a fixed offshore wind turbine. In: Proc. of the World Renewable Energy Congress XI; 2010.

[23] Oskamp JA, Ozkan-Haller HY. Power calculations for a passively tuned Point absorber wave energy converter on the Oregon coast. Renew Energy 2012;42:72–7.
[24] Zanuttigh B, Angelelli E, Kofoed JP. Effects of mooring systems on the performance of a wave activated body energy converter. Renew Energy 2013;57:422–31.
[25] Sjolte J, Bjerke IK, Tjensvoll G, Molinas M. Summary of performance after one year of operation with the Lifesaver Wave Energy Converter System. In: Proc. of the 10th European Wave and Tidal Energy Conference, Aalborg, Denmark; 2013.
[26] de Andrés AD, Guanche R, Vidal C, Losada IJ. Analysis of the geometric tunability of a WEC from a worldwide perspective. In: Proc. of the 33rd International Conference on Ocean, Offshore and Artic Engineering, San Francisco, California, USA; 2014.
[27] Neary V, Previsic M, Jepsen RA, Lawson MJ, Yu Yi-Hsiang, Copping AE, et al. Methodology for design and economic analysis of marine energy conversion (MEC) technologies. 2014. Technical report from Sandia National Laboratories (USA), SAND2014–9040.
[28] Skyner D. Solo duck linear analysis. Technical Report. University of Edinburgh; 1987.
[29] Folley M, Whittaker TJT, Henry A. The effect of water depth on the performance of a small surging wave energy converter. Ocean Eng 2007;34:1265–74.
[30] Flocard F, Finnigan TD. Experimental investigation of power capture from pitching point absorbers. In: Proc. 8th European Wave and Tidal Energy Conference, Uppsala, Sweden; 2009.
[31] Henry A, Doherty K, Cameron L, Whittaker T, Doherty R. Advances in the design of the oyster wave energy converter. In: Proc. Royal Institution of Naval Architects Marine and Offshore Renewable Energy Conference; 2010.
[32] Pecher A, Kofoed JP, Larsen T. Design specifications for the WEPTOS Hansthom WEC. Energies 2012;5(4):1001–17.
[33] Pecher A, Kofoed JP, Larsen T, Marchalot T. Experimental study of the WEPTOS wave energy converter. In: Proc. of the 21st International Conference on Ocean, Offshore and Artic Engineering, Rio de Janeiro, Brazil; 2012.
[34] Pecher A, Kofoed JP, Larsen T. The extensive R&D behind the Weptos WEC. In: Proceedings of the 1st International Conference on Renewable Energies Offshore (RENEW2014), Lisbon, Portugal; 2014.
[35] Renzi E, Dias F. Resonant behaviour of an oscillating wave energy converter in a channel. J Fluid Mech 2012;701:482–510.
[36] Soulard T, Babarit A, Borgarino B. Estimation de la production d'une plateforme flottante hybride pour la récupération de l'énergie des vagues et du vent. In: Proc. of the 13emes Journees de l'hydrodynamique, Chatou, France; 2012.
[37] Soulard T, Babarit A, Borgarino B. Preliminary assessment of a semi-submersible floating wind turbine combined with pitching wave energy converters. In: Proc. of the 10th European Wave and Tidal Energy Conference, Aalborg, Denmark; 2013.
[38] Gomes RPF, Lopes MFP, Henriques JCC, Gato LMC, Falcao AFO. The dyrnamics and power extraction of bottom-hinged plate wave energy converters in regular and irregular waves. Ocean Eng 2015;96:86–99.
[39] Pecher A, Kofoed JP, Espedal J, Hagberg S. Results of an experimental study of the Langlee Wave Energy Converter. In: Proc. of the 20th International Offshore and Polar Engineering Conference, Beijing, China; 2010.
[40] Lavelle J, Kofoed JP. Experimental testing of the Langlee Wave Energy Converter. In: Proc. of the 9th European Wave and Tidal Energy Conference, Southampton, UK; 2011.
[41] Angelelli E, Zanuttigh B, Kofoed JP, Glejbol K. Experiments on the WavePiston Wave Energy Converter. In: Proc. of the 9th European Wave and Tidal Energy Conference, Southampton, UK; 2011.
[42] Cordonnier J, Gorintin F, De Cagny A, Clement AH, Babarit A. SEAREV: case study of the development of a wave energy converter. Renew Energy 2015;80:40–52.
[43] Rendel Palmer, Tritton, Kennedy, Donkin. United Kingdom wave energy program – Consultants' 1981 assessment. UK: Department of Energy; 1982.
[44] Yu Y-H, Li Y, Hallett K, Hotimsky C. Design and analysis for a floating oscillating surge wave energy converter. In: Proc. of the 33rd International Conference on Ocean, Offshore and Artic Engineering, San Francisco, California, USA; 2014.
[45] Kamizuru Y. Development of hydrostatic drive trains for wave energy converters. PhD thesis. Aachen University; 2014.
[46] Falnes J. A resonant point absorber of ocean-wave power. Nature 1975;256:478–9.
[47] Babarit A, Clement AH. Application of the optimal command method to the control of the SEAREV wave energy converter: a study on the influence of time constants on the efficiency of the latching control. In: Proc of the 9th European Control Conference, Budapest, Hungary; 2009.
[48] Cretel J, Lewis AW, Thomas G, Lightbody G. A critical assessment of latching as control strategy for wave-energy absorbers. In: Proc.. of the 31st International Offshore and Polar Engineering Conference, Hawaii; 2011.
[49] Genest R, Bonnefoy F, Clement AH, Babarit A. Effect of non ideal power take off one the energy absorption of a reactively controlled one degree of freedom wave energy converter. Appl Ocean Res 2014;48:236–43.
[50] Evans DV. A theory for wave-power absorption by oscillating bodies. J Fluid Mech 1976;77(1):1–25.
[51] Stansell P, Pizer DJ. Maximum wave-power absorption by attenuating line absorbers under volume constraints. Cornwell University Library; 2011.
[52] Grases JM. MARINET Infrastructure access report. Infrastructure: IFREMER Deep Seawater Wave Tank. User-project: SDK Wave Turbine. 2013.
[53] Prasad DD, Ahmed MR, Lee Y-H. Flow and performance characteristics of a direct drive turbine for wave power generation. Ocean Eng 2014;81:39–49.
[54] Farley FJM, Rainey RCT, Chaplin JR. Rubber tubes in the sea. Philos Trans R Soc A 2012;370:381–402.
[55] Babarit A, Gendron B, Singh J, Mélis C, Jean P. Hydro-elastic modelling of an electro-active wave energy converter. In: Proc. of the 32nd International Conference on Ocean, Offshore and Artic Engineering, Nantes, France; 2013.
[56] Ramboll, Dansk Hydraulisk Institut, Danmarks meteorologiske institut. Kortlaegning af bolgeenergiforhold i den Danske del af nordsoean. 1999. Technical report. In Danish.
[57] Verdel T. Décision et prévision statistiques. Chapitre 7: la régression linéaire. 2007. Lecture notes of Ecole des Mines de Nancy. In French.
[58] Gunn K, Stock-Williams C. Quantifying the global wave power resource. Renew Energy 2012;44:296–304.